Supporting Information

Specific detection of hypochlorite based on size-selective effect of luminophore integrated MOF-801 synthesized by a one-pot strategy

Yunxi Ye,[a] Liwei Zhao,[a] Shuanggang Hu,[b] Ajuan Liang,[b]* Yongsheng Li,[a] Qixin Zhuang,[a] Guorong Tao[c]* and Jinlou Gu[a]*

[a] Key Laboratory for Ultrafine Materials of Ministry of Education, School of Materials Science and Engineering, East China University of Science and Technology, Shanghai 200237, China. Email: jinlougu@ecust.edu.cn

[b] Center for Reproductive Medicine, Renji Hospital, School of Medicine, Shanghai Jiao Tong University, Shanghai Key Laboratory for Assisted Reproduction and Reproductive Genetics, Shanghai 200135, China. Email: amao1977@163.com

[c] Department of Anesthesiology, Ruijin Hospital, Shanghai Jiaotong University School of Medicine, Shanghai 200025, China. Email: zjsxtgr@126.com

Fax: +86-21-64250740; Tel: +86-21-64252599

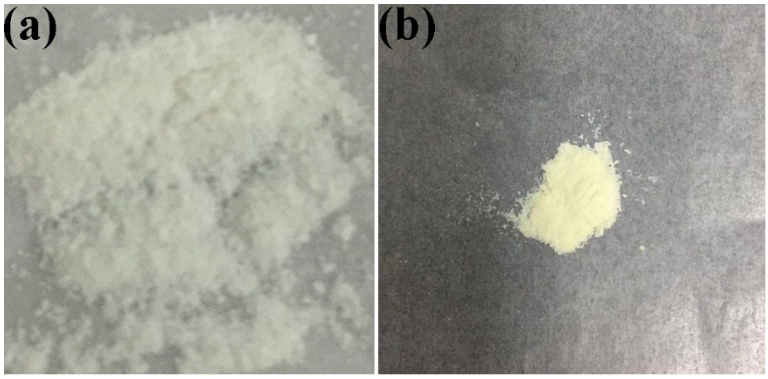

Fig. S1 Digital photographs of the (a) MOF-801 and (b) AF@MOF-801 NPs.

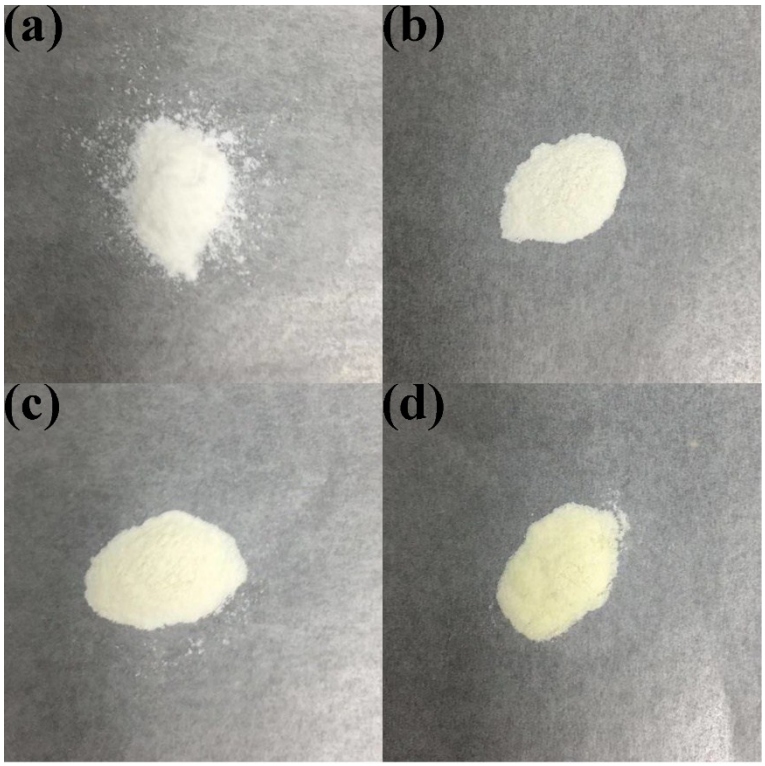

Fig. S2 Digital photographs of AF@MOF-801 NPs with AF/FUM feed ratios of (a) 0.024:1, (b) 0.096:1, (c) 0.144:1 and (d) 0.216:1.

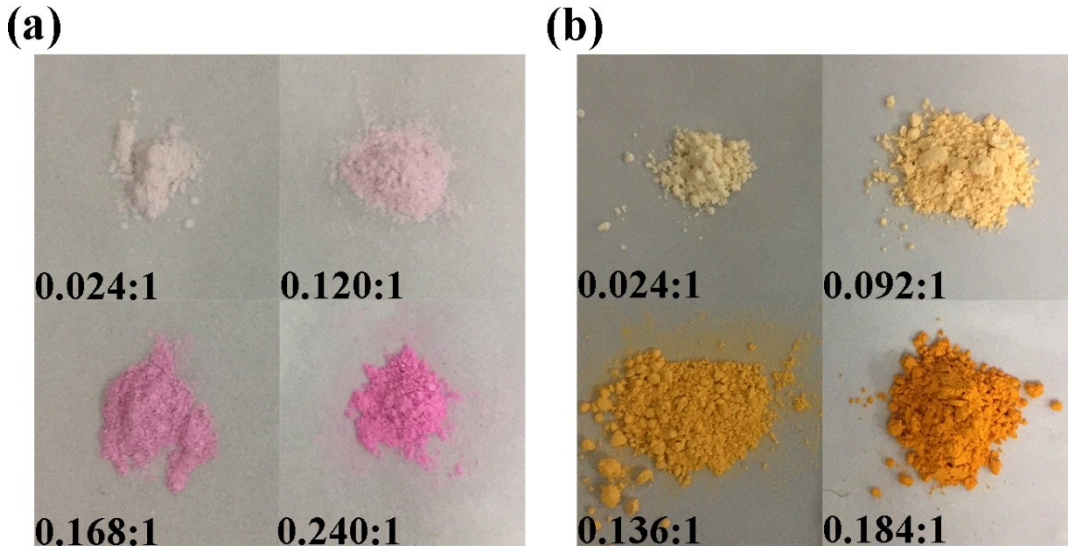

Fig. S3 Digital photographs of (a) RhB@MOF-801 and (b) calcein@MOF-801 NPs with different RhB/FUM feed ratio from 0.024:1 to 0.240:1 and calcein/FUM of 0.024:1 to 0.184:1.

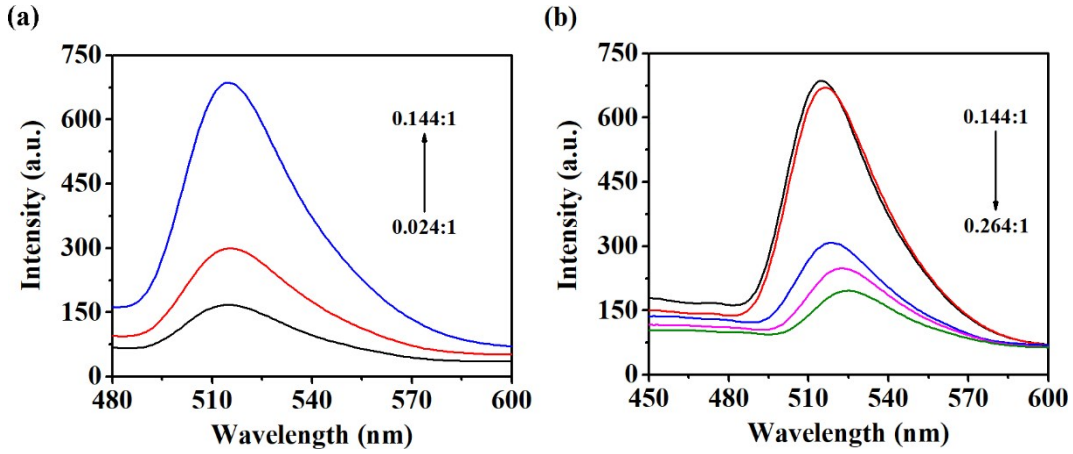

Fig. S4 The fluorescence evolvement curves of AF@MOF-801 NPs with different AF/FUM feed ratios of (a) from 0.024 :1 to 0.144 :1 and (b) from 0.144 : 1 to 0.264 :1.

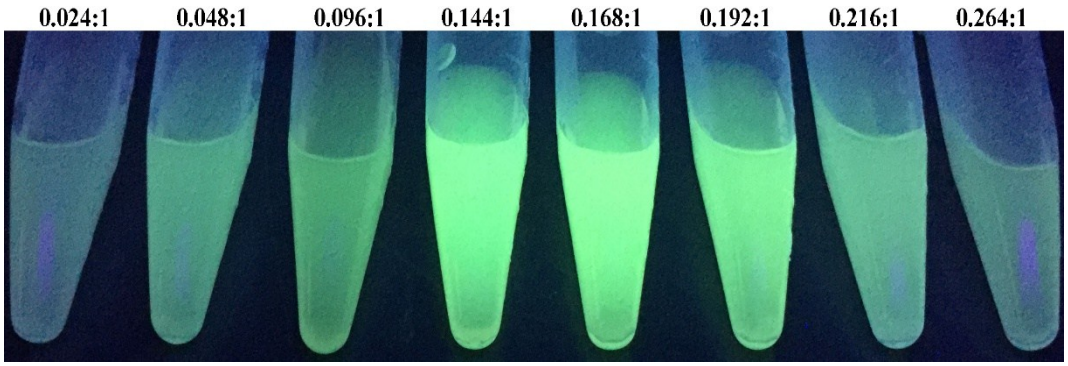

Fig. S5 The fluorescence photographs of AF@MOF-801 NPs with different AF/FUM feed ratio from 0.024:1 to 0.262:1. The fluorescence was excited with a UV lamp.

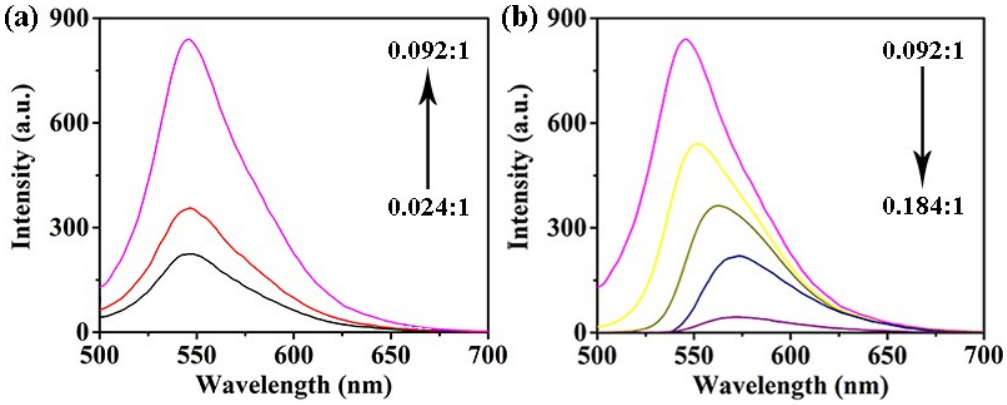

Fig. S6 The fluorescence evolvement curves of calcein@MOF-801 NPs with different calcein/FUM feed ratios of (a) from 0.024:1 to 0.092:1 and (b) from 0.092:1 to 0.184:1.

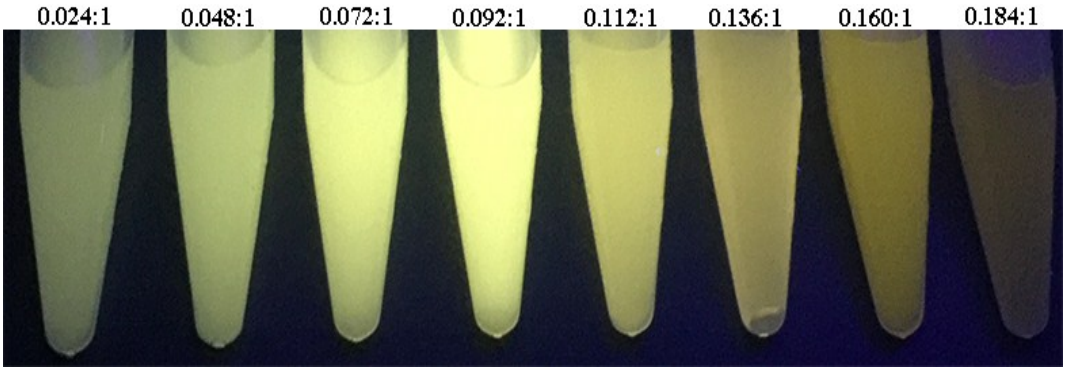

Fig. S7 The fluorescence photographs of calcein@MOF-801 NPs with different calcein/FUM feed ratio from 0.024:1 to 0.184:1. The fluorescence was excited with a UV lamp.

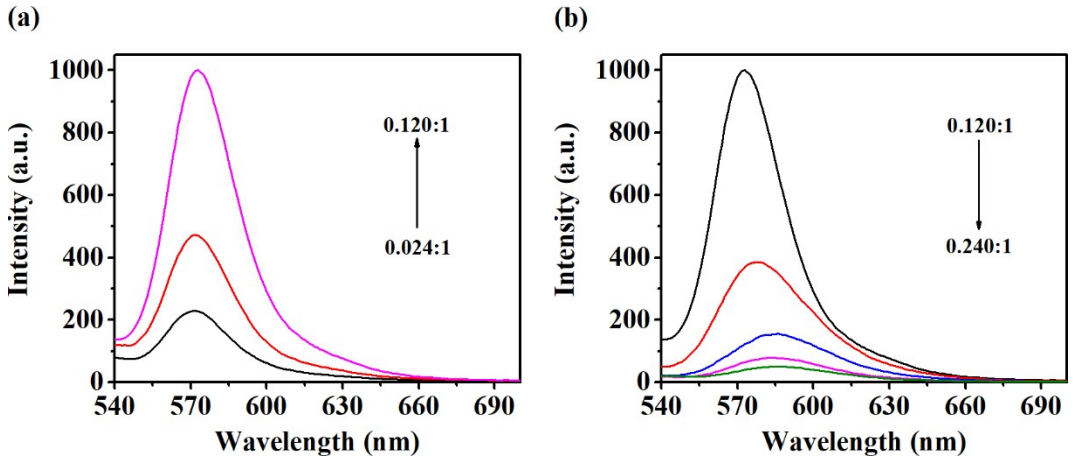

Fig. S8 The fluorescence evolvement curves of RhB@MOF-801 NPs with different RhB/FUM feed ratios of (a) from 0.024:1 to 0.120:1 and (b) from 0.120:1 to 0.240:1.

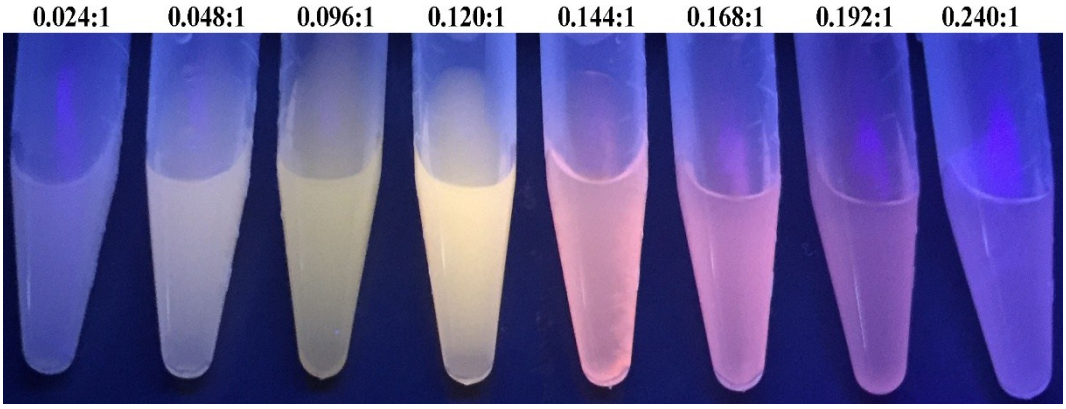

Fig. S9 The fluorescence photographs of RhB@MOF-801 NPs with different RhB/FUM feed ratio from 0.024:1 to 0.240:1. The fluorescence was excited with a UV lamp.

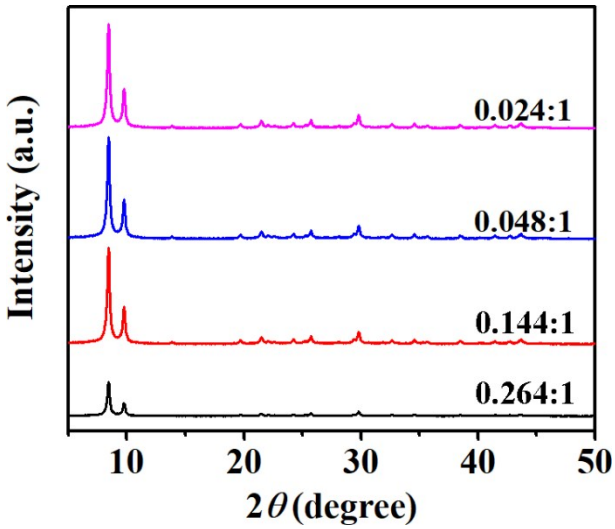

Fig. S10 The XRD patterns of AF@MOF-801 NPs with different AF/FUM feed ratios from 0.024:1 to 0.264:1.

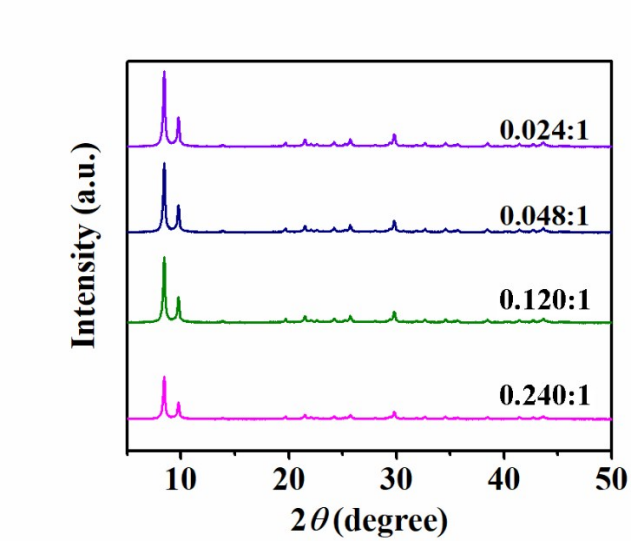

Fig. S11 The XRD patterns of RhB@MOF-801 NPs with different RhB/FUM feed ratios from 0.024:1 to 0.240:1.

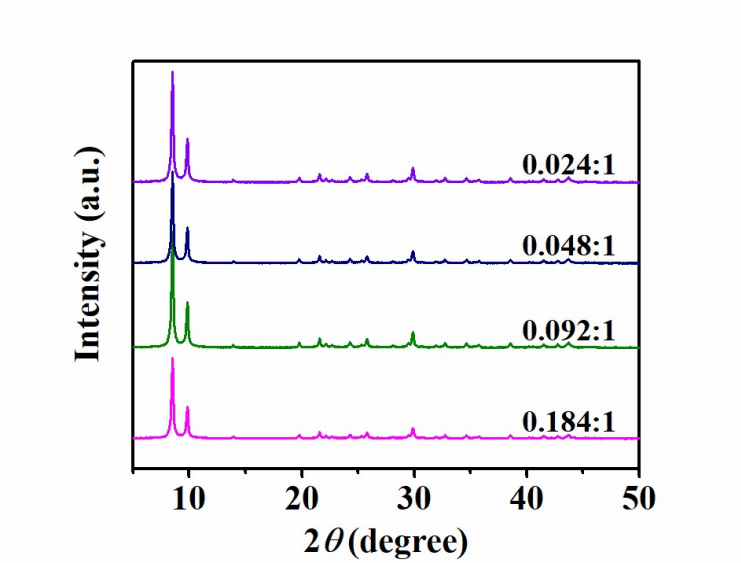

Fig. S12 The XRD patterns of calcein@MOF-801 NPs with different calcein/FUM feed ratios from 0.024:1 to 0.184:1.

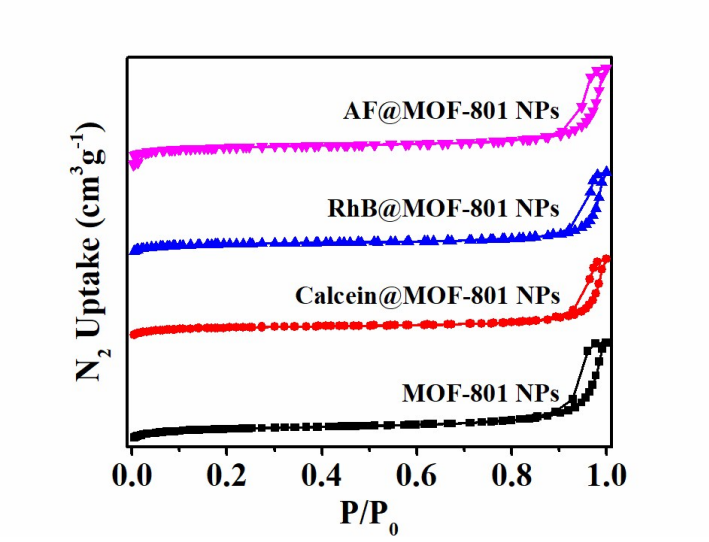

Fig. S13 The N_2 adsorption/desorption isotherms of blank MOF-801, RhB@MOF-801, calcein@MOF-801 NPs and AF@MOF-801 NPs recorded at 77 K.

Table S1. Textural parameters of the synthesized pure MOF-801 NPs, RhB@MOF-801 NPs, calcein@MOF-801 NPs and AF@MOF-801 NPs.

Materials	BET surface area ($m^2 g^{-1}$)	Total pore volume ($cm^3 g^{-1}$)
pure MOF-801 NPs	936.7	0.78
RhB@MOF-801 NPs	851.5	0.72
calcein@MOF-801 NPs	811.5	0.66
AF@MOF-801 NPs	870.2	0.73

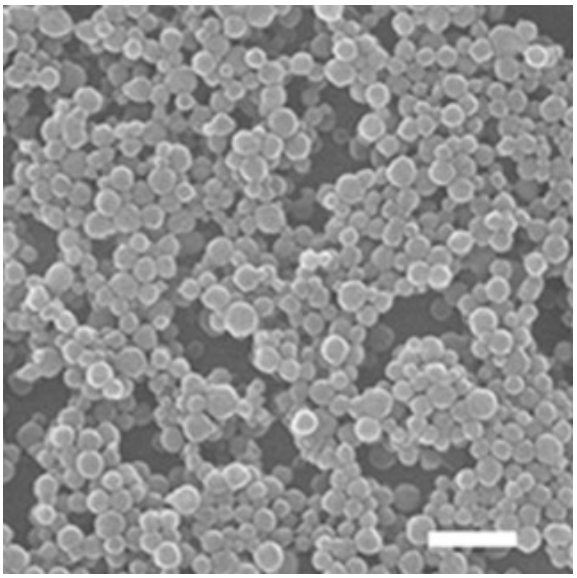

Fig. S14 The SEM image of RhB@MOF-801 NPs (scale bar: 200 nm). The feed ratio of RhB/FUM was set as 0.120:1.

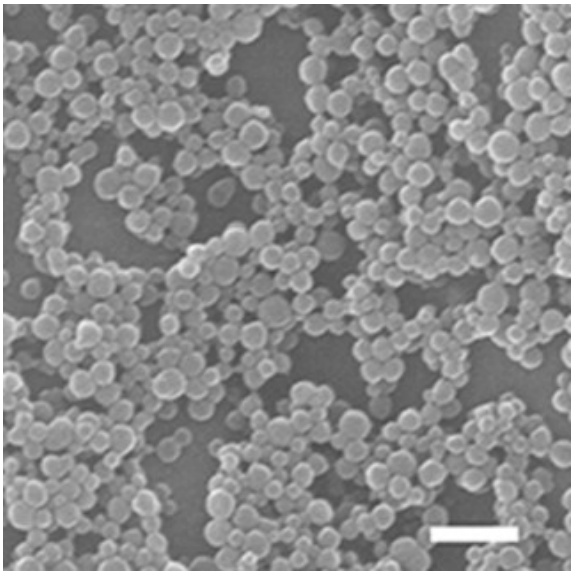

Fig. S15 The SEM image of calcein@MOF-801 NPs (scale bar: 200 nm). The feed ratio of calcein/FUM was set as 0.092:1.

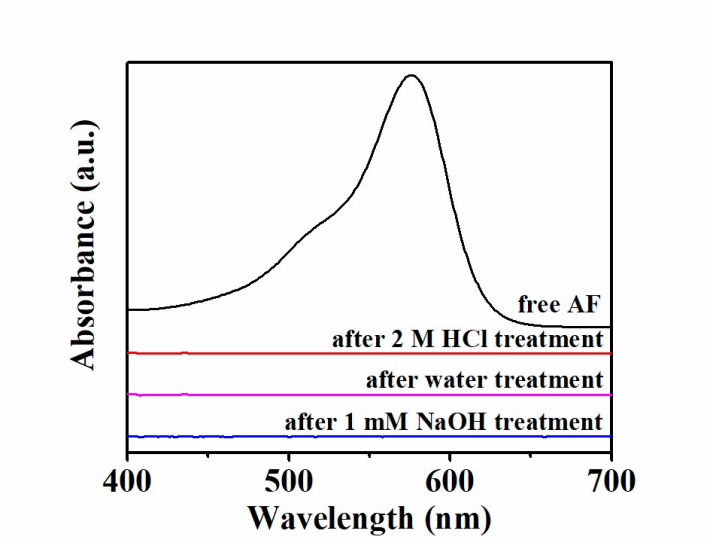

Fig. S16 The UV-vis spectra of the supernatant decanted from AF@MOF-801 NPs suspension after different treatments. The free AF molecule was dissolved in an ethanol-water (mass ratio of 5:95) mixture solution.

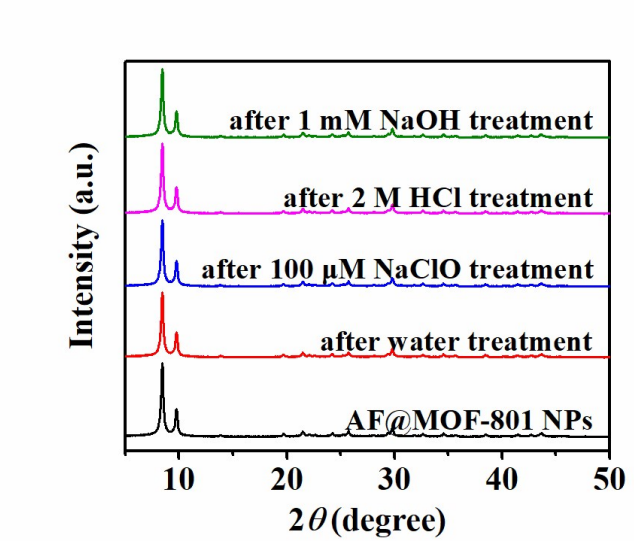

Fig. S17 The XRD patterns of AF@MOF-801 NPs before (black) and after treatment with water (red), NaClO (blue), HCl (pink) and NaOH (green) solutions for 12 h.

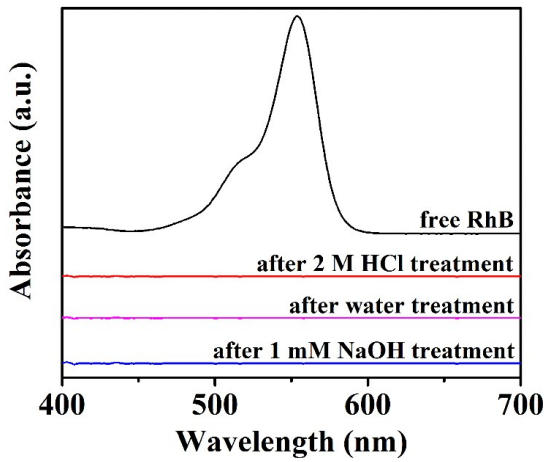

Fig. S18 The UV-vis spectra of the RhB@MOF-801 NPs supernatant after treatment with water (pink), HCl (red) and NaOH (blue) solutions. Free RhB molecules were dissolved in the ultrapure water.

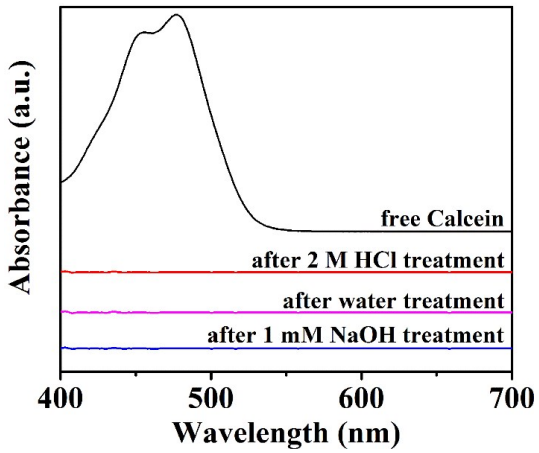

Fig. S19 The UV-vis spectra of the calcein@MOF-801 NPs supernatant after treatment with water (pink), HCl (red) and NaOH (blue) solutions. Free calcein molecules were dissolved in the ultrapure water.

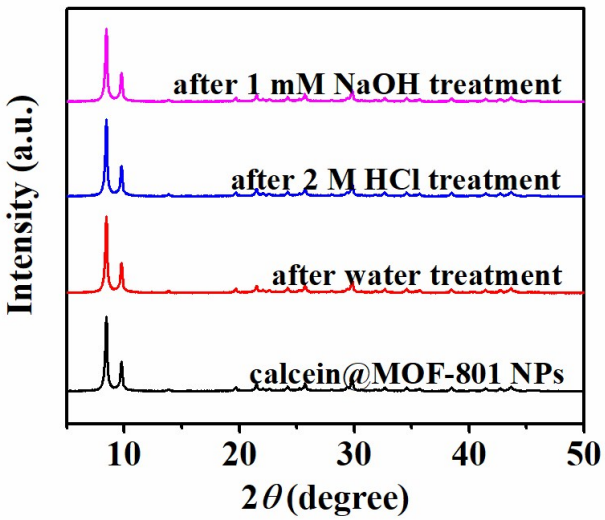

Fig. S20 The XRD patterns of calcein@MOF-801 NPs before (black) and after treatment with water (red), HCl (blue) and NaOH (pink) solutions for 12 h.

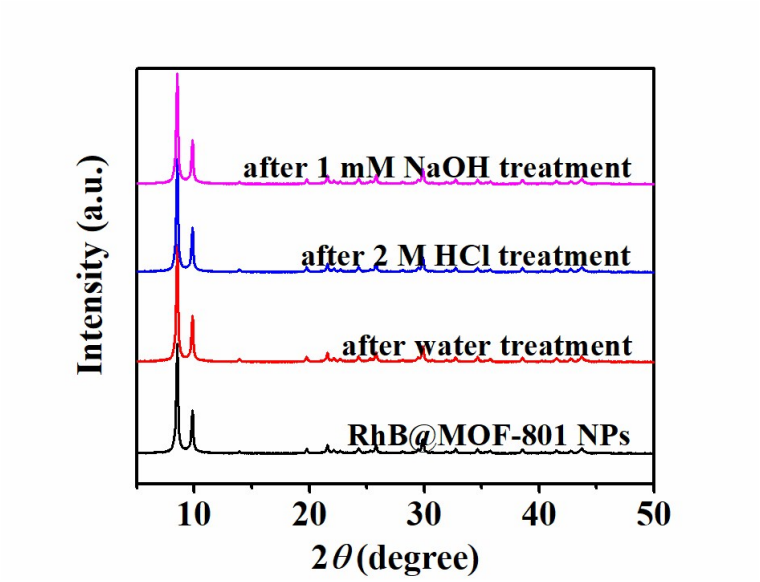

Fig. S21 The XRD patterns of RhB@MOF-801 NPs before (black) and after treatment with water (red), HCl (blue) and NaOH (pink) solutions for 12 h.

The calculation method for the LOD of AF@MOF-801 NPs toward ClO^- detection in aqueous phase at pH=7.4.

$$\text{Detection Limit} = 3\sigma/\text{slope}$$

$$= 3\times 1.18/68.44$$

$$= 0.05172\ \mu M$$

Luminescent spectrum was recorded for the blank sample of AF@MOF-801 NPs suspension. Sample standard deviation of σ for the blank probe without the addition of ClO^- was calculated to be 1.18 at pH = 7.4.

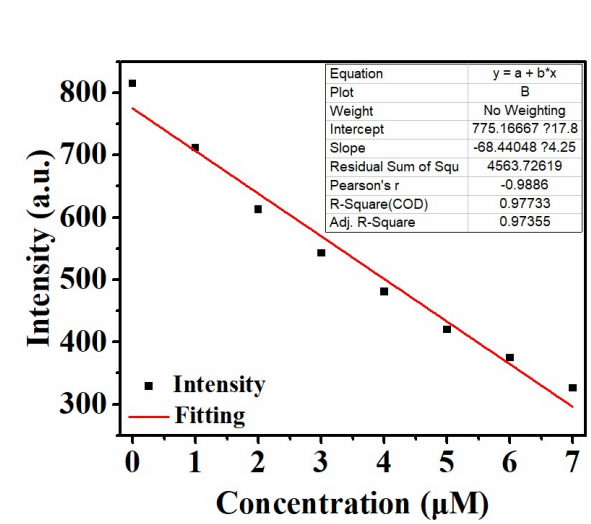

Fig. S22 The relation of luminescent intensity against ClO^- added into AF@MOF-801 NPs suspension and their linear fit curve for the estimation of LOD at pH= 7.4.

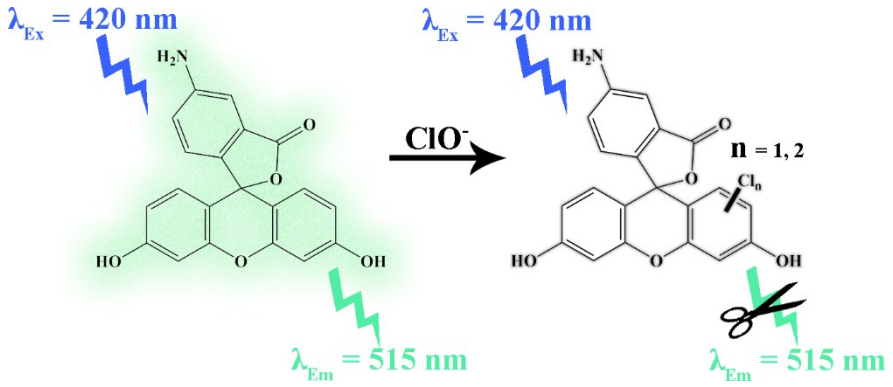

Scheme S1 Schematic illustration for the quenching mechanism of AF for ClO^- detection.

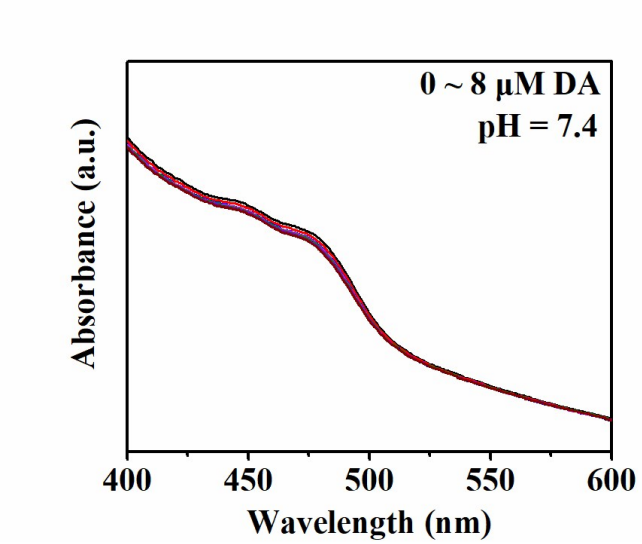

Fig. S23 The UV-vis spectra of the AF@MOF-801 NPs supernatant upon the addition of DA with its concentration range from 0 to 8 μM at pH = 7.4.

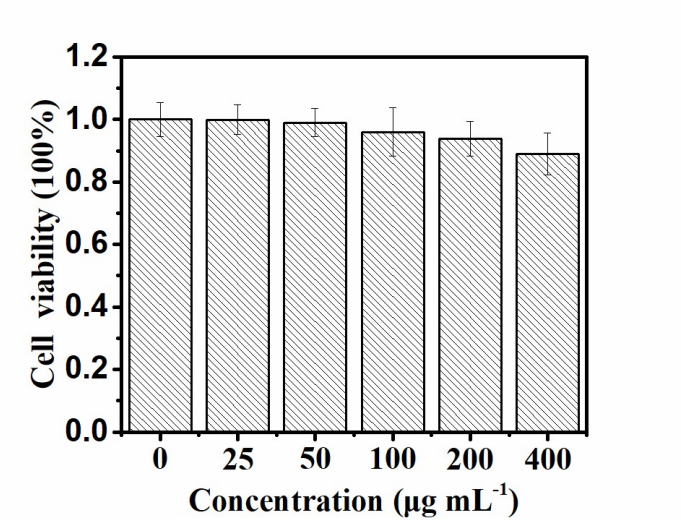

Fig. S24 The cell viability of SMMC-7721 cells incubated with different concentrations of the AF@MOF-801 NPs. Untreated control cells were used as a reference.

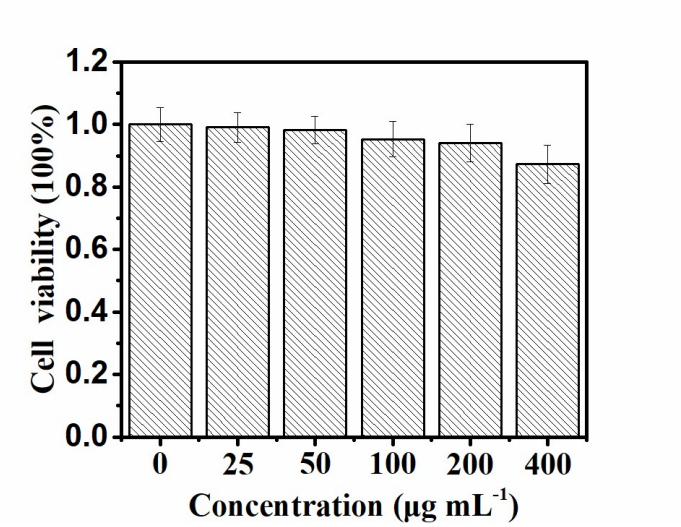

Fig. S25 The cell viability of HeLa cells incubated with different concentration of the AF@MOF-801 NPs. Untreated control cells were used as a reference.

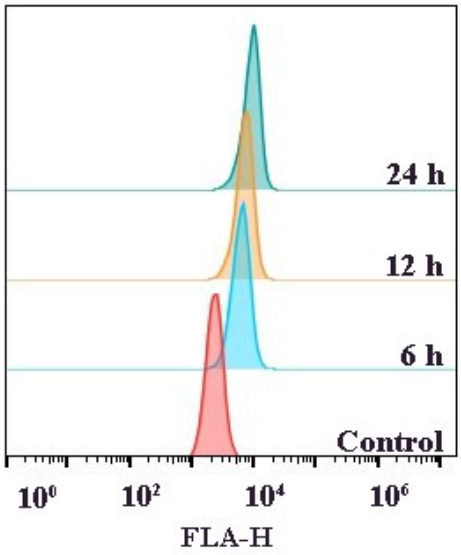

Fig. S26 The flow cytometry histograms of SMMC-7721 cells incubated with the AF@MOF-801 NPs within 0 to 24 h. Untreated control cells were used as a control group.

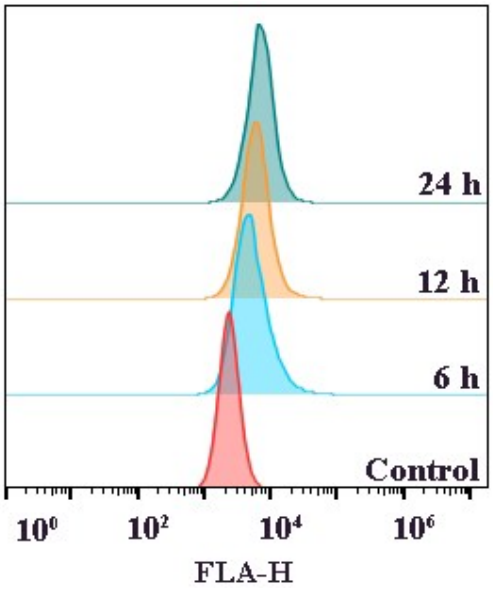

Fig. S27 The flow cytometry histograms of HeLa cells incubated with the AF@MOF-801 NPs within 0 to 24 h. Untreated control cells were used as a control group.

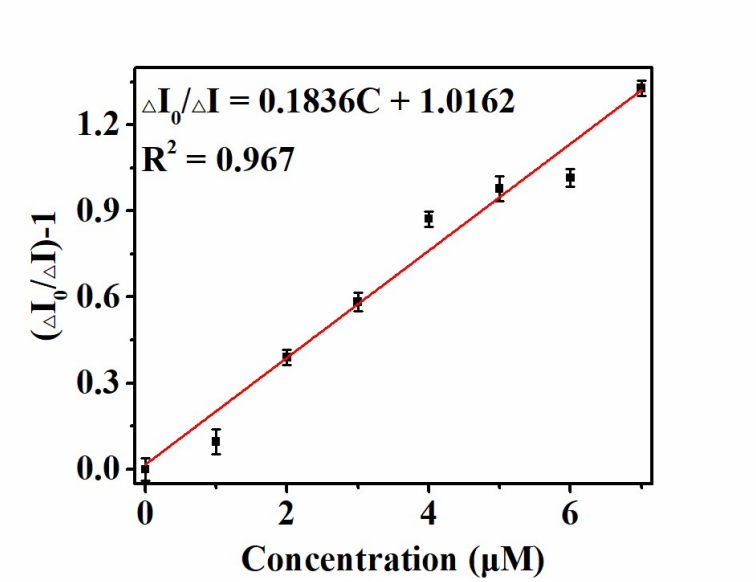

Fig. S28 The concentration-response curve of luminescence decrease of AF@MOF-801 NPs in SMMC-7721 cells after 30 min exposure to various concentrations of ClO^- donors. ΔI was obtained by subtracting the luminescence intensity of control group from the real-time luminescence intensity. Each datum point represents the mean of datum from eight wells (n=8) with error bars and the untreated cells were used as control. The concentration of the AF@MOF-801 NPs probe was set as 50 μg mL^{-1}.

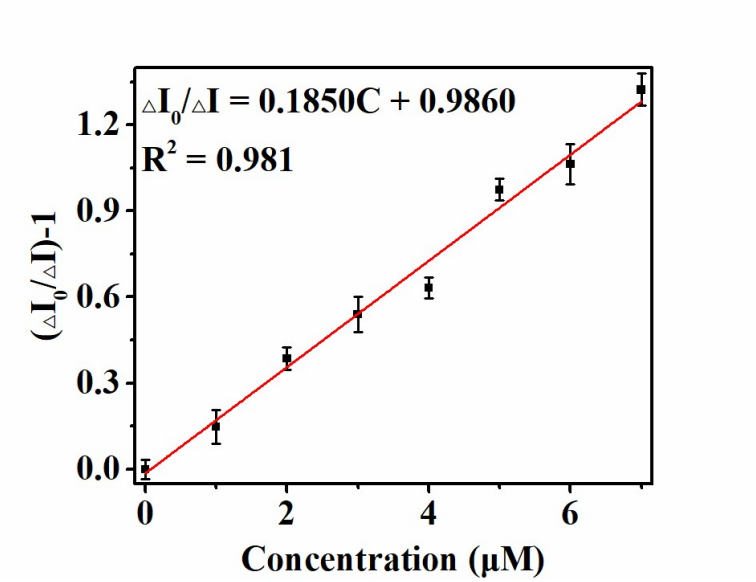

Fig. S29 The concentration-response curve of luminescence decrease of AF@MOF-801 NPs in HeLa cells after 30 min exposure to various concentrations of ClO^- donors. ΔI was obtained by subtracting the luminescence intensity of control group from the real-time luminescence intensity. Each datum point represents the mean of datum from eight wells (n=8) with error bars and the untreated cells were used as control. The concentration of the AF@MOF-801 NPs probe was set as 50 μg mL^{-1}.

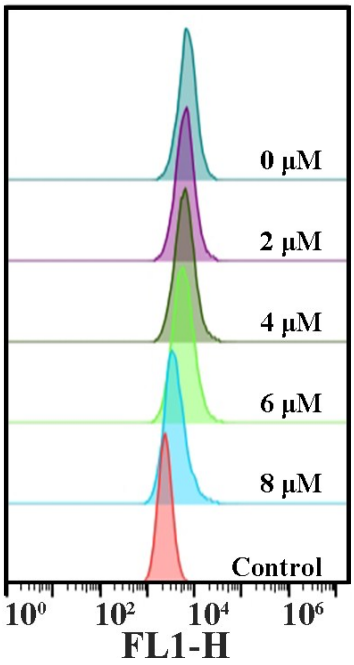

Fig. 30 The Flow cytometry histograms of the AF@MOF-801 NPs in HeLa cells after 30 min exposure to various concentrations of ClO^-. Untreated cells were used as control. The concentration of the AF@MOF-801 NPs probe was set as 50 μg mL^{-1}.

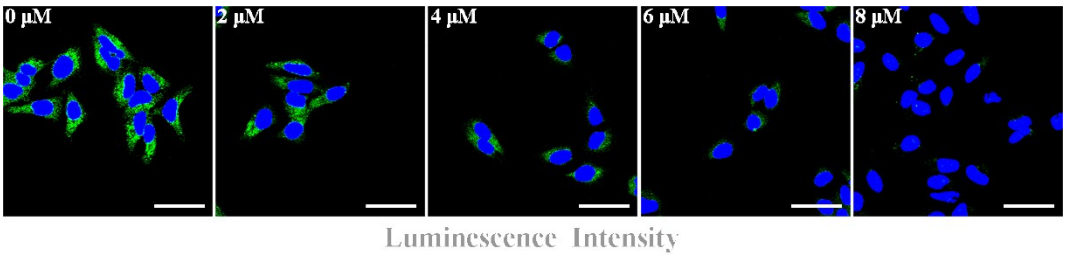

Fig. 31 The CLSM images of HeLa cells cultured at 37 ℃ with AF@MOF-801 NPs for 12 h and then incubated with various concentrations of ClO^- (scale bar: 50 μm). The concentration of the AF@MOF-801 NPs probe was set as 50 μg mL^{-1}.